THE PUBLISHING HOUSE
OF THE ROMANIAN ACADEMY

PROCEEDINGS OF THE ROMANIAN ACADEMY, Series A,
Volume 15, Number 2/2014, pp. 208–215

DETECTION OF ELECTROMAGNETIC WAVES WITH A SINGLE CARBON ATOM SHEET

Mircea DRAGOMAN

National Institute for Research and Development in Microtechnology (IMT), P.O. Box 38-160, 023573 Bucharest, Romania

The aim of this paper is to show that simple devices based on graphene monolayer devices are able to detect electromagnetic fields in an amazing large spectrum ranging from microwaves up to far IR.

Key words: graphene, microwave, optics.

1. INTRODUCTION

The graphene monolayer is a single atom sheet with a thickness of 0.34 nm consisting of carbon atoms in the sp^2 hybridization state. The physical properties of the graphene monolayer are displayed in Table 1.

Table 1

The physical properties of graphene

Parameter	Values	Comments
Mobility	40 000 $cm^2V^{-1}s^{-1}$	At room temperature (intrinsic mobility 200 000 $cm^2V^{-1}s^{-1}$ in suspended structures)
Mean free path (ballistic transport)	200- 300 nm	At room temperature
Fermi velocity	$c/300$ = 1000000 m/s	At room temperature
Thermal conductivity	5 000 W/mK	Better thermal conductivity than in most crystals
Young modulus	1.5 Tpa	Ten times greater than in steel
Mobility	40 000 $cm^2V^{-1}s^{-1}$	At room temperature (intrinsic mobility 200 000 $cm^2V^{-1}s^{-1}$ in suspended structures)

We will present here neither the physics nor the methods of obtaining graphene in details, which are presented elsewhere [1]. However, some basic aspects must be underlined. The graphene monolayer is a 2D material, in deep contrast with any other material, which is 3D. The transport of carriers in graphene is described by the Dirac equation in place of the Schrödinger equation as in any other material. This fact is generating the amazing properties that are encountered in graphene. From the transport point of view the dispersion relation in graphene is given by $E = \pm\hbar\,|\,\boldsymbol{k}\,|\,v_F$, where $\boldsymbol{k} = \boldsymbol{i}k_x + \boldsymbol{j}k_y$ is the wavevector measured from the Dirac points K or K' in the reciprocal space, v_F is the Fermi velocity of 10^6 m/s, and the positive or negative sign is associated to electrons or holes. This transport equation is represented by two cones, as shown in Fig. 1.

The Fermi level in graphene, which is usually position at the Dirac point, can be tuned by a gate voltage and in this way we are able to select a certain type of carriers in graphene. All devices based on graphene are ambipolar, i.e. they can work based on either electrons or holes. In graphene, electrons and holes have the same physical properties, in contrast to any semiconductors. The graphene monolayer, as well as symmetric bilayer graphene sheets, has no bandgap, but multilayer graphene has band gaps.

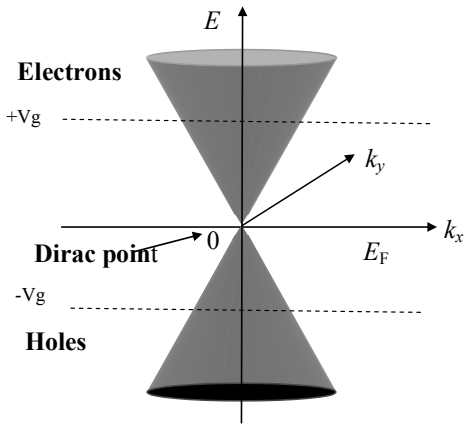

Fig. 1 –The graphene dispersion.

The graphene has very high carrier mobility and a very large mean-free path at room temperature allowing the fabrication of ballistic devices with nanoscale dimensions able to work at room temperature. The zero effective mass of carriers in graphene monolayers signifies the ballistic nature of charge carriers around Dirac points. Much more details about the transport properties of graphene monolayers are found in [2]. The transport properties of graphene is now well studied and well understood.

In contrast, the electromagnetic properties of graphene in RF, microwave, and millimeter waves are not well known and not well exploited. Coplanar (CPW) metallic lines deposited on graphene (which is deposited on Si/SiO_2, the thickness of SiO_2 being 300 nm) were designed and fabricated and it was demonstrated that graphene is working as a DC-voltage-tunable matching device [3], and that the contact resistance – a serious issue in graphene – is shorted beyond few GHz. In this way, graphene devices are performing contactless in measurements up to 110 GHz [4]. It is established that electromagnetic propagation in graphene is nonlinear [5]. The interaction between graphene and optical fields starts to be better understood and exploited [6].

2. DETECTION OF ELECTROMAGNETIC WAVES IN THE MICROWAVE SPECTRUM BASED ON GRAPHENE

The detection of electromagnetic waves in the microwave spectrum implies a nonlinear device able to demodulate a microwave field and an antenna. Initially, we have worked with a very simple graphene device –a CPW line on graphene (Fig. 2)

The CPW on graphene is fabricated on a high-resistivity (greater than 8 kΩ) Si substrate, on which 300 nm of SiO_2 is grown by thermal oxidation. The graphene monolayer deposition on the Si/SiO_2 substrate was performed by Graphene Industries. Then, the CPW consisting of three parallel gold metallic electrodes (the central conductor is the signal electrode and the outer conductors are ground electrodes) was patterned.

The gold electrodes were deposited over the graphene monolayer using the fabrication process based on e-beam patterning developed in [7]. Large microwave pads were connected to both ends of the CPW to be able to connect CPW graphene with the probe station (Karl-Suss PM5).

DC and microwave measurements were made on the device represented in Fig. 3. We did not use an antenna coupled to the CPW on graphene, but a microwave generator having the carrier frequency signal in the frequency range 100 MHz – 25 GHz, which excites the CPW on graphene. The generator has the ability to modulate the carrier signal with AM modulation having a spectrum in the audio frequency range. A low – noise amplifier (LNA) (Stanford Research SR560) followed by a digital oscilloscope (Tektronix, SR560) is located at the other output of the CPW on graphene, to display the demodulated signal (Fig. 3). Figure 3a is a radio-like configuration for CPW on graphene.

The DC response of the CPW on graphene can be modeled by the formula:

$$I = I_0[\exp(V / V_0) - 1]. \tag{1}$$

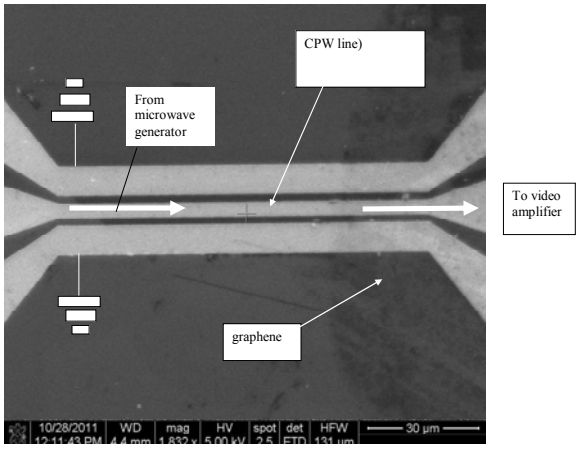

Fig. 2 – The CPW on graphene as a nonlinear element for detecting radiowaves (Reproduced with permission from Appl. Phys. Lett. **109**, pp. 033109/1-3, 2012, copyright 2012 AIP Publishing LLC.)

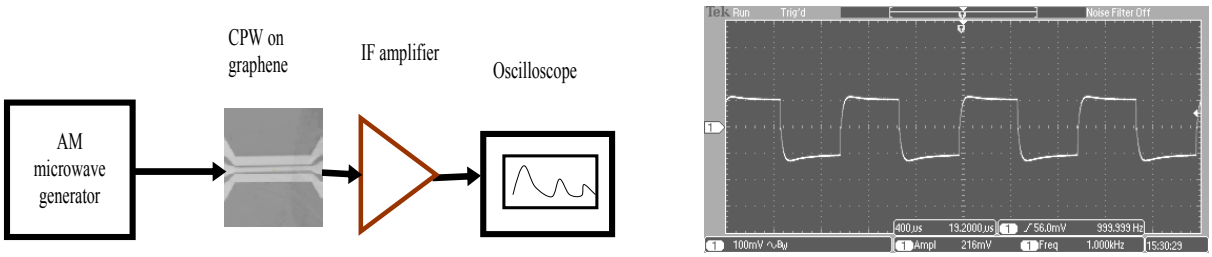

(a) (b)

Fig. 3 – a) A radio-like configuration measurement for CPW on grapheme; b) the 1 kHz signal detected by the radio. (Reproduced with permission from Appl. Phys. Lett. **109**, pp. 033109/1-3, 2012, copyright 2012 AIP Publishing LLC.)

From the experimental *I–V* dependence we have found, by fitting the data, that the parameters I_0 and V_0 have values of 3.65 mA and 4.68 V, respectively, for the positive polarization. In the case of negative polarization we found that I_0 and V_0 are –2.6 mA and –3.12 V. The *I–V* dependence is strongly nonlinear and will be used for electromagnetic field detection.

The analytic formula (1) is used to find the demodulated signal, which is considered to be the second-order term in the Taylor series expansion of the current near the operating point, at which $I = I_{av}$, $V = V_{av}$. Thus, we have:

$$I - I_{av} = I_0 \frac{(V - V_{av})^2}{2V_0^2} \exp(V_{av} / V_0) . \tag{2}$$

The demodulating signal is then given by $(I - I_{av})R_l$, where $R_l = 50\ \Omega$.

In all our experiments we have used the 0 dBm of the generator in the entire spectrum between 100 MHz and 25 GHz. We have obtained a maximum responsivity of our graphene radio of 1100 V/W at 3.5 GHz, which is impressing for a single carbon sheet. Also, the experimental data confirms the analytic formula (2). More details about the measurements of this graphene radio are found in [8]. No radio based on semiconductors is able to work in such a large bandwidth. An example of DC detection of the 1 kHz audio signal is displayed in Fig. 3b.

After obtaining the result presented above, two questions arise: could we have a nonlinear graphene device at the wafer scale? Could we have also a graphene antenna, to be able to have an integrated receiver antenna diode grown on wafer? We will try briefly to explain the progress done up to now in this respect.

Recently, we have found a ballistic diode able to rectify the signal only due to its geometric shape, which in our case is a trapezoidal shape. The theory of this diode is presented in [9] and the fabrication process, as well as the first experimental results, is reported in [10].

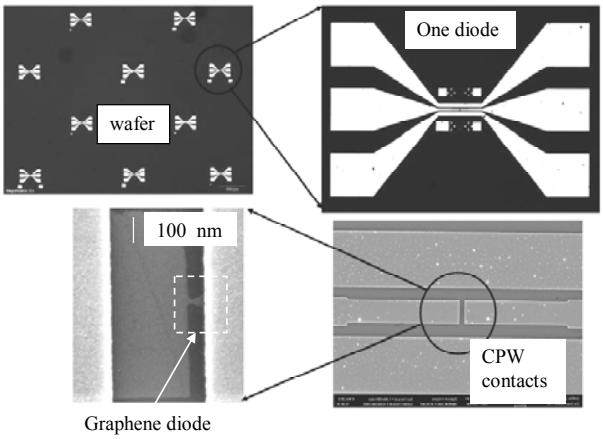

Fig. 4 – The graphene "fannel" diode on wafer.

The SEM photo in Fig. 4 illustrates a graphene ballistic diode having a length of 100 nm. The diode shoulder has a width of d_{in} = 100 nm and a neck width of only d_{out} = 30 nm. A Keithley 4200 SCS equipment is employed for DC measurements of several diodes on the same wafer (Fig. 4). The *I–V* curves as a function of the back-gate voltage are displayed in Fig. 5. A zero current range of 140 mV is observed centered around 0 V. At low gate voltages of ± (10 V–20 V) the current is sharply augmented, but the zero current area is well conserved and the diode is rectifying. A different situation happens at high gate voltages (–40 V–60 V). There are many electrons interacting between them, the ballistic transport regime is lost and the diode works like an electron funnel, i.e. the current is becoming constant since too many electrons are flowing in a 30 nm width diode neck.

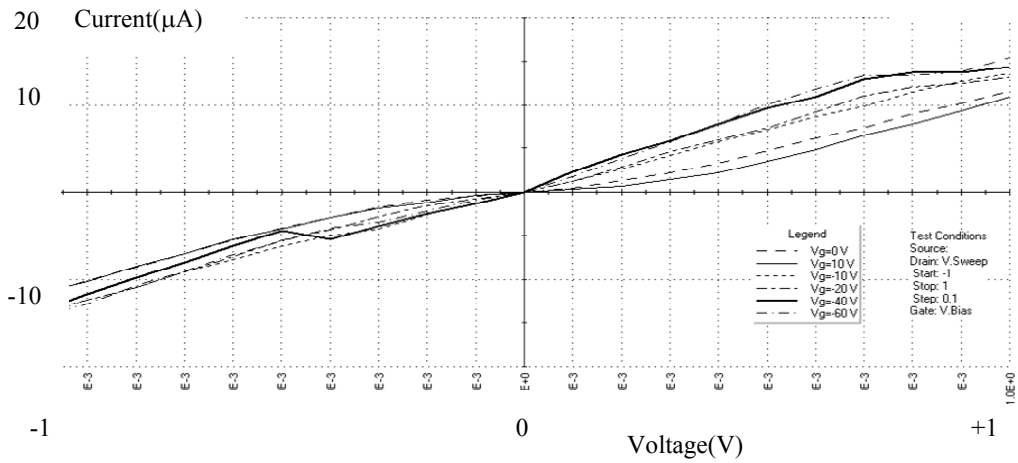

Fig. 5 – The current-voltage dependence.

The above graphene ballistic diode integrated with an antenna works with a responsivity of 21.4 V/W up to 10 THz, which is an amazing value for any electronic device [11]. This effort is in the promising direction of using graphene to detect THz waves [12], with the final goal to have integrated circuits beyond 200 GHz up 10 THz, especially for imaging applications [13].

The graphene antennas are in infancy. The first efforts were done only in the last years. A graphene slot-patch antenna is displayed in Fig. 6a. In spite of the high surface graphene resistance (200–700 Ω) the CST simulations have shown that graphene antenna are efficient. Defining *S* as the gap width between the graphene layer and ground electrodes, *A* as the CPW hot wire width, *B* as the CPW gap between the hot wire and the ground electrode, and considering S = 450 μm, A = 100 μm, B = 50 μm and R_s = 250 Ω, we have displayed in Fig. 6b, the simulated S11 parameter of the graphene antenna. We see that the antenna has a resonance at 9.53 GHz. At this resonant frequency the radiation pattern and the efficiency are represented in Fig. 7.

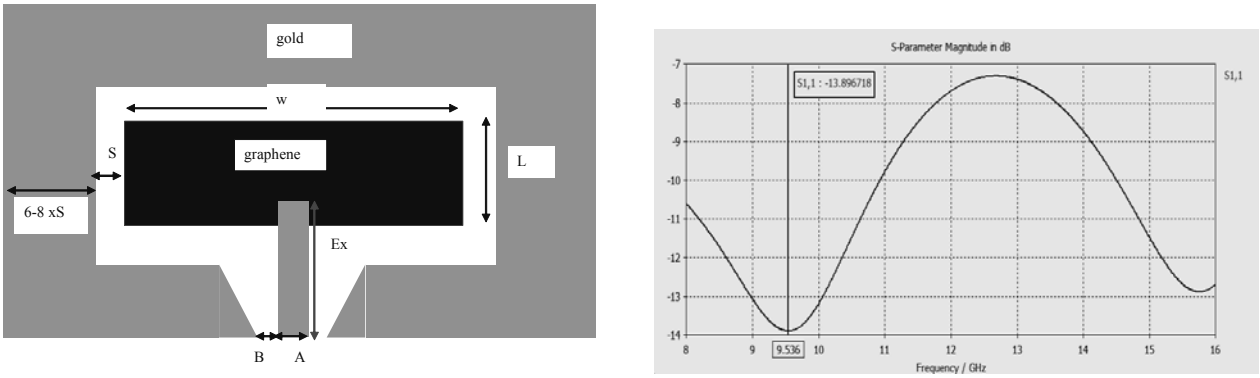

(a) (b)

Fig. 6 – a) Graphene antenna; b) S11 of the graphene antenna.

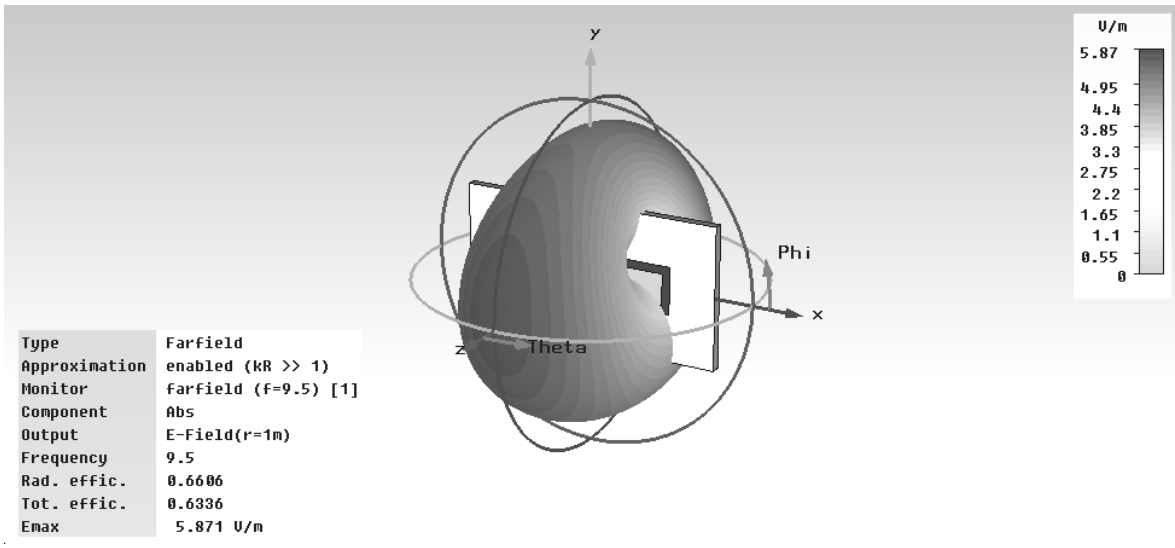

Fig. 7 – The graphene radiation pattern.

The total efficiency is 63%, which is not at all a small value. This high efficiency could be the advantage of such an antenna compared to a slot-patch antenna on the same Si/SO_2 ground.

The conductivity in graphene has two components: intraband and interband conductivities [14]:

$$\sigma = \sigma_{\text{intra}} + \sigma_{\text{inter}} . \tag{3}$$

The intraband term is expressed as:

$$\sigma_{\text{intra}} = -ie^2 k_B T / \pi\hbar^2 (\omega - i2\Gamma) \times \{(\mu_c / k_B T) + 2\ln[\exp(-\mu_c / k_B T) + 1]\} . \tag{4}$$

where $\mu_c \cong e\alpha V_b$ is the chemical potential, with α a geometry-dependent constant and V_b the bias voltage (a value of 0.13 eV was chosen for μ_c in the simulations). T is the temperature – the room temperature is 300 K, and $\Gamma = 11$ meV. The intraband term dominates the graphene conductivity over an ultrawideband of frequencies, from DC up to 1 THz [15], the real part of the intraband conductivity being much larger than the imaginary part in this frequency range.

Thus, the surface impedance of the graphene antenna is tunable as a function of the DC bias applied on graphene and we have:

$$Z_S(V_b) = 1/\sigma(\omega) = R_s(V_b) + \mathrm{j}X_s(V_b) , \tag{5}$$

meaning that S11 as well as the radiation pattern is tunable via a DC voltage. This fact will be exploited in the near future for innovative antennas.

3. DETECTION OF ELECTROMAGNETIC WAVES IN THE OPTICAL SPECTRUM BASED ON GRAPHENE

Graphene is the only material which, in a huge spectral bandwidth encompassing terahertz (THz) [16], infrared (IR) [17] and visible (VIS) [18] radiation, has an amazing optical property, i.e. a frequency-independent absorption given by $A \cong (2.3 \pm 0.2)\% \cong (1 \pm 0.1)\pi\alpha$, where α is the fine structure constant. These data suggest that we could be able to fabricate a photodetector based on graphene having a huge bandwidth, from ultraviolet up to near infrared, i.e. in the bandwidth 200–2500 nm, which is an unparallel photodetector because it exceeds with many orders of magnitude the bandwidth of existing photodetectors.

In this respect, we have used graphene ink from Nanointegris consisting of pure graphene flakes soluble in water. We have functionalized these graphene flakes with nanoparticles of Au and Ag to enhance the photoresponse via plasmonics resonances, and bovine serum albumine was added to get a uniform deposition over an interdigitated electrode (IDT). The IDT is a 24 gold pair electrode deposited on SiO_2 thermally grown on a high-resistive Si. The width of the electrode is 3 μm, while the distance between two consecutive electrode fingers is only 1 μm. The solution of graphene ink or functionalized graphene is deposited over the IDT in a very small quantity, of 100 nL. The chemical functionalization, measurement techniques and results are presented in [19]. We note here that it is not easy at all to measure optical characteristics in the very large wavelength range of 200–2500 nm. We have used lamps and their characteristics are described in [19]. The best results were obtained using graphene functionalized with Ag nanoparticles. The responsivity is displayed in Fig. 8. We see that in near IR we have the best results, of 13.7 mA/W.

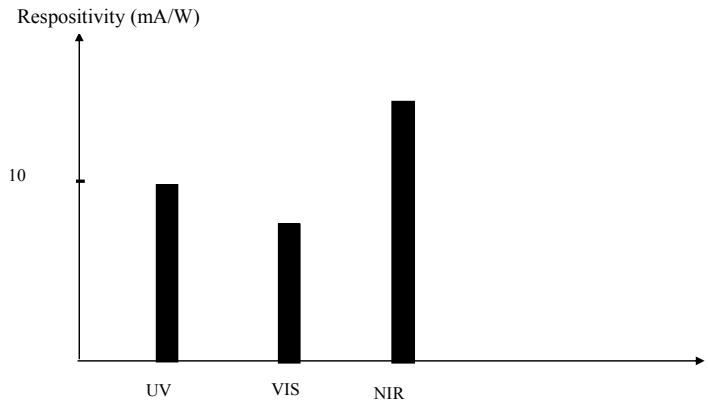

Fig. 8 – The responsivity of the graphene photodetector.

The above results are with one order of magnitude greater than the first graphene photodetector having the responsivity of 0.5 mA/W and developed by an IBM team using a graphene FET [20]. However, the best result for 2D materials is obtained using MoS_2 flakes. Here, at the wavelength of 561 nm, the responsivity is 850 A/W [21]. However, it remains to demonstrate whether MoS_2 is able to provide such a large bandwidth as graphene.

Very recently, we have shown that a CPW deposited on high resistivity *n*-Si, having the central electrode as an IDT formed by Au/Pt electrodes and further covered with graphene ink functionalized with gold nanoislands is working as: (i) photodetector, (ii) solar cell, depending on how we connect the input and output electrodes. When (i) the two ends of the IDT are connected and biased, a wide band photodetector with a good responsivity is obtained, while (ii) when the IDT is connected with any other outer electrode, the device is acting as a solar cell with an efficiency of 0.8% [22]. Both phenomena are explained by the Schottky contact between graphene and Si used first for carbon nanotube solar cells [23] and then used in graphene cells [24, 25]. The CPW has as ground electrodes two large Au electrodes encompassing the IDT central electrode and having the following dimensions: the length of an electrode is L = 100 μm, its width is 3 μm, and the distance between two consecutive electrodes is 1 μm. The metal thickness is 300 nm. On this coplanar IDT array we have deposited 200 nL of graphene ink (having the surfactant removed as described in [22]) decorated with gold nanoislands, as shown in Fig. 9a.

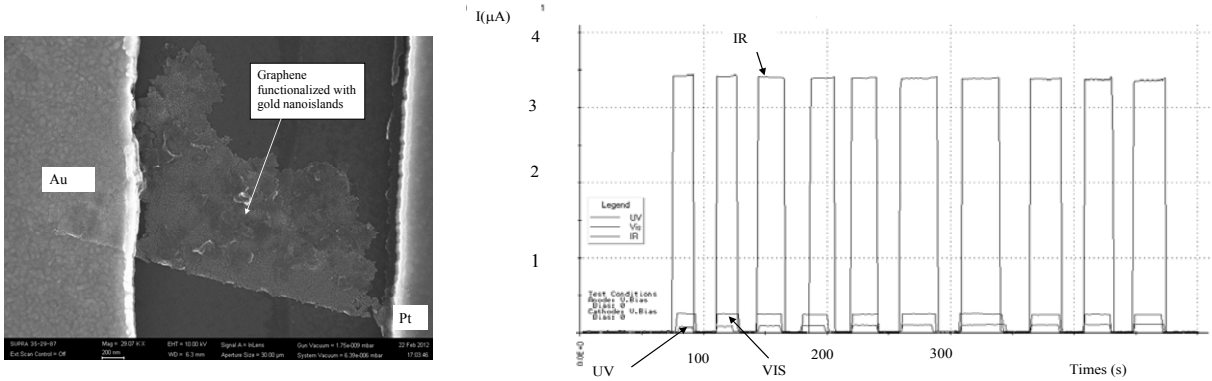

(a) (b)

Fig. 9 – a) Detail of the IDT central electrode: graphene ink functionalized with Au nanoislands; b) sensing of light in the UV, VIS and IR without applied DC.

Again, as in the first example, a couple of optical lamps were used to study the photodetection properties of the device shown in detail in Fig. 9a. This time, the responsivity in the IR is 30 mA/W, which after our knowledge is the state-of-the-art value. The time response of switching ON-and-OFF the UV, VIS and IR light sources is presented in Fig. 9b in the absence of a DC voltage. We see the fast response of the graphene device and the fact that IR is the predominant response. We note that these DC pulses are generated only due to the action of light on graphene ink functionalized with gold nanoparticles.

4. CONCLUSIONS

I have reviewed here a part of my work in the last years. It was hard to believe that such a tiny material formed by a single sheet of carbon atoms – graphene – is able to detect electromagnetic radiation having wavelength much higher than its dimensions. The paper shows the advancement of graphene technology starting from graphene exfoliated via scotch method up to graphene on wafer, and graphene functionalized with nanoparticles, nanoislands etc. The graphene future is bright due to its many applications in nanoelectronics, nanotechnology and other areas.

ACKNOWLEDGEMENTS

I would like to thank many scientists which helped me in the quest in the area of carbon nanoelectronics, most of them being co-authors of many papers published in the last period of time. My wife Daniela has helped me with her deep knowledge in the area of quantum mechanics, solid state physics and graphene physics. My colleagues from IMT Bucharest (Adrian Dinescu,Alex Muller, Dan Neculoiu, Alina Cismaru, Antonio Radoi), dr. George Konstantinidis from FORTH Heraklion, dr. George Deligeorgis from LAAS Toulouse were behind almost any device reported in this talk especially due to their invaluable knowledge in the area of semiconductor technology. This work was supported by a grant of Romanian National Authority for Scientific Research, CNCS-UEFISCDI, project number PN-II-ID-PCE-2011-3-0071, and FP 7 NANO RF (grant agreement 318352)

REFERENCES

1. M. Dragoman, D. Dragoman, *Graphene-based quantum electronics*, Progr. Quantum Electronics, **33**, pp. 165-214, 2009.
2. A.H. Castro-Neto, F. Guinea, N.M.R. Peres, K.S. Novoselov, A.K. Geim, *The electronic properties of graphene*, Rev. Mod. Phys., **81**, pp. 109–162, 2009.
3. M. Dragoman, D. Neculoiu, A. Cismaru, A.A. Müller, G. Deligeorgis, G. Konstantinidis, D. Dragoman, R. Plana, *Coplanar waveguide on graphene in the range 40 MHz–110 GHz*, Appl. Phys. Lett., **99**, pp. 033112/1–3, 2011.

4. H.S. Skulason, H.V. Nguyen, A. Guermoune, V. Sridharan, M. Siaj, C. Caloz, T. Szkopek, *110 GHz measurement of large-area graphene integrated in low-loss microwave structures*, Appl. Phys. Lett., **99**, pp. 153504/1–3, 2011.
5. S.A. Mikhailov, *Electromagnetic response of graphene: Non-linear effects*, Physica E, **40**, 2626–2629 (2008).
6. Q. Bao, K.P. Loh, *Graphene photonics, plasmonics, and broadband optoelectronic devices,* ACS Nano, **6**, pp. 3677–3694, 2012.
7. M. Dragoman, D. Dragoman, G. Deligeorgis, G. Konstantinidis, D. Neculou, A. Cismaru, R. Plana, *Current oscillations in a wide graphene sheet*, J. Appl. Phys., **106**, pp. 044312/1–4, 2009.
8. M. Dragoman, D. Neculoiu, A. Cismaru, G. Deligeorgis, G. Konstantinidis, D. Dragoman, *Graphene nanoradio: Detecting radiowaves with a single atom sheet*, Appl. Phys. Lett., **109**, pp. 033109/1–3, 2012.
9. D. Dragoman, M. Dragoman, *Geometrically induced rectification in two-dimensional ballistic nanodevices*, J. Phys., D **46**, pp. 055306/1–6, 2013.
10. M. Dragoman, A. Dinescu, D. Dragoman, *On-wafer graphene diodes for high-frequency applications*, European Solid State Device Research Conference (ESSDERC), Bucharest, September 2013, pp. 322–324.
11. M. Dragoman, M. Aldrigo, A. Dinescu, D. Dragoman, A. Constanzo, *Towards a terahertz direct receiver based on graphene up to 10 THz*, J. Appl. Phys., in press, 2014.
12. L. Vicarelli, M.S. Vitiello, D. Coquillat, A. Lombardo, A.C. Ferrari, W. Knap, M. Polini, V. Pellegrini, A. Trediccuci, *Graphene field–effect transistors as room temperature terahertz detectors*, Nature Materials, **11**, pp. 865–871, 2012.
13. B. Sensale-Rodriguez, S. Rafique, R. Yan, M. Zhu, V. Protasenko, D. Jena, L. Liu, H.G. Xing, *Terahertz imaging employing graphene modulator arrays*, Optics Express, **21**, pp. 2324–2330, 2013.
14. G.W. Hanson, *Dyadic Green's function and guided surface waves for a surface conductivity model of graphene,* J. Appl. Phys., **103**, pp. 064302/1–5, 2008.
15. S. Rodríguez, R. Yen, L. Liu, D. Jena, H.G. Xiang, *Graphene for reconfigurable terahertz optoelectronics,* Proc., IEEE, **101**, pp. 1705–1716, 2013.
16. J.W. Dawlaty, S.S. Shivaraman, J. Strait, P. George, M. Chandrashekhar, F. Rana, M.G. Spencer, D. Veksler, Y. Chen, *Measurement of the optical spectra of epitaxial graphene from terahertz up to visible,* Appl. Phys. Lett., **93**, pp. 131905/1–3, 2010.
17. K.F. Mak, M.Y. Sfeir, Y. Wu, C.H. Lui, J.A. Misewich, T.F. Heinz, *Measurement of the optical conductivity of graphen*e, Phys. Rev. Lett., **101**, pp. 196405/1–4, 2008.
18. R.R. Nair, P. Blake, A.N. Grigorenko, K.S. Novoselov, T.J. Boot, T. Stauber, N.M.R. Peres, A.K. Geim*, Fine structure constant defines visual transparency of graphene*, Science, **320**, p. 1308, 2010.
19. A. Radoi, A. Iordanescu, A. Cismaru, D. Dragoman, M. Dragoman, *Ultrabroadband photodetection based on graphene ink*, Nanotechnology, **21**, pp. 455202/1–5, 2010.
20. F. Xia, T. Mueller, Y.-M. Lin, A. Valdes-Garcia, P. Avouris, *Utrafast graphene photodetector*, Nature Nanotechnology, **4**, pp. 839–843, 2009.
21. O. Lopez-Sanchez, D. Lemke, M. Kayci, A. Radenovic, A. Kis, *Ultrasensitive photodetectors based on monolayer* MoS_2, Nature Nanotechnology, **8**, pp. 497–501, 2013.
22. A. Radoi, M. Dragoman, A. Cismaru, G. Konstantinidis, D. Dragoman, *Self-powered microwave devices based on graphene ink decorated with gold nanoislands,* J. Appl. Phys., **112**, pp. 064327/1–4, 2012.
23. Y. Jia, J. Wei, K. Wang, A. Cao, Q. Shu, X. Gui, Y. Zhu, D. Zhang, G. Zhang, B. Ma, L.Wang, W. Liu, Z. Wang, J. Luo, D. Wu*, Nanotube-silicon heterojunction solar cells*, Adv. Mat., **20**, pp. 4594–4598, 2008.
24. X. Li, H. Zhu, K. Wang, A. Cao, J. Wei, C. Li, Y. Jia, Z. Li, D. Wu, *Graphene-on silicon Schottky solar cell*, Adv. Mater., **22**, pp. 2743–2748, 2010
25. T. Feng, D. Xie, Y. Liu, Y. Zang, T. Ren, R. Song, H. Zhao, H. Tian, X. Li, H. Zhu, L. Liu, *Graphene based Schottky junction solar cells on patterned silicon-pillar array substrate*, Appl. Phys. Lett., **99**, pp. 233505/1–3, 2011.

Received February 3, 2014